ADVANCED FUNCTIONAL MATERIALS
www.afm-journal.de

All-in-One Iontronic Sensing Paper

Sen Li, Ning Pan, Zijie Zhu, Ruya Li, Baoqing Li, Jiaru Chu, Guanglin Li, Yu Chang, and Tingrui Pan**

Paper has been utilized as an ideal platform for chemical, biological, and mechanical sensing for its fibrous structures and properties in addition to its low cost. However, current studies on pressure-sensitive papers have not fully utilized the unique advantages of papers, such as printability, cuttability, and foldability. Moreover, the existing resistive, capacitive, and triboelectric sensing modalities have long-standing challenges in sensitivity, noise-proofing, response time, linearity, etc. Here, a novel flexible iontronic sensing mechanism, referred to as iontronic sensing paper (ISP), is introduced to the classic paper substrates by incorporating both ionic and conductive patterns into an all-in-one flexible sensing platform. The ISP can then be structured into 2D or 3D tactile-sensitive origamis only by the paper-specific manipulations of printing, cutting, folding, and gluing. Notably, the ISP device possesses a device sensitivity of 10 nF kPa^{-1} cm^{-2}, which is thousands of times higher than that of the commercial counterpart, a resolution of 6.25 Pa, a single-millisecond response time, and a high linearity ($R^2 > 0.996$). Benefiting from the unique properties of the fibrous paper structures and its remarkable performances, the ISP devices hold enormous potential for the emerging human–machine interfaces, including smart packaging, health wearables, and pressure-sensitive paper matrix.

1. Introduction

Paper, made of natural or artificial cellulose fibers with additives, has evolved throughout human history and played a very important role in our daily life, primarily to record and spread information. Being a soft, foldable, printable, cuttable, disposable, degradable material at a low cost, paper has long been utilized as a flexible platform for chemical and biological sensing. For instance, the pH papers, blood glucose-sensing strips, and early pregnancy detection kits are the most notable ones, along with the recent developments of organic gas sensors, DNA and protein sensors, and heavy ion detection devices.[1–15] Furthermore, benefiting from their fibrous structure, papers can be modified with functional additives, such as carbon-derived materials (e.g., carbon nanotube (CNT) and graphene), conductive polymers, and metallic nanocomposites, leading to new functionalities and sensing modalities.[16–21] Among these emerging functional papers, pressure-sensitive papers can be configured with a simple device architecture due to its straightforward sensing principles.[22–25] Although recent studies have successfully exhibited the device flexibility, low-cost manufacturability, and disposability, the additional unique natural advantages of paper have not been fully utilized, such as printability, cuttability, and foldability.

The previously reported pressure-sensitive papers, along with the pressure sensors made of them are primarily based on three existing sensing mechanisms, i.e., resistive, capacitive, and triboelectric.[22,26,27] The resistive pressure-sensing papers detect the variations of the electrical resistance induced by the change of the contact area between two resistor structures upon the applied pressure, which can be prepared by dip coating and spray coating of a particular conductive material. Ren's group has reported a novel graphene paper prepared by immersing tissue papers into a graphene oxide solution, and consecutively, this paper pressure sensing device has exhibited a sensitivity of 17.2 kPa^{-1} within the range of 2 kPa.[22] Cheng's group has published a gold nanowire coated paper as a functional sensing material, the prepared pressure sensing device shows a device sensitivity of 1.14 kPa^{-1} within the range of 5 kPa.[25] However, the nonlinearity between the resistance measurements and the pressure readings can lead to substantial reduction in the device sensitivity as pressure increases. For instance, the sensitivity of the graphene-paper pressure sensor dramatically declines from 17.2 to 0.012 kPa^{-1} beyond its range limit of 2 kPa, thus restricting its practical utilities and applications.[22] Alternatively, the capacitive pressure-sensitive papers typically utilize parallel electrodes sandwiching a compressible dielectric layer.[28–30] As the loading pressure increases, the distance between two parallel

S. Li, Prof. G. Li, Dr. Y. Chang
Bionic Sensing and Intelligence Center (BSIC)
Institute of Biomedical and Health Engineering
Shenzhen Institutes of Advanced Technology
Chinese Academy of Science
1068 Xueyuan Avenue, Shenzhen 518055, China
E-mail: yu.chang@siat.ac.cn
S. Li, Prof. B. Li, Prof. J. Chu
Department of Precision Machinery and Precision Instrumentation
University of Science and Technology of China
96 Jinzhai Road, Hefei 230027, China
Prof. N. Pan, Dr. Z. Zhu, Prof. R. Li, Dr. Y. Chang, Prof. T. Pan
Micro-Nano Innovations (MINI) Laboratory
Department of Biomedical Engineering
University of California
Davis, One Shields Avenue, Davis, CA 95616, USA
E-mail: trpan@ucdavis.edu
The ORCID identification number(s) for the author(s) of this article can be found under https://doi.org/10.1002/adfm.201807343.

DOI: 10.1002/adfm.201807343

paper electrodes decreases, resulting in the rise of the capacitance. However, such sensing capacitance are typically measured in the order of tens to hundreds of pF, which can be easily influenced by environmental conditions, in particular, parasitic-induced capacitive noises (on the same order of magnitude), leading to reduced device accuracy and stability.[31] Finally, the recent development on the triboelectric sensing papers employ the triboelectric effect to measure pressure variations applied to the sensors. Wang's group has reported a paper sensing device incorporating a triboelectric polytetrafluoroethylene (PTFE) film and a silver-coated paper substrate.[24] Although it is highly sensitive to dynamic pressure changes, the triboelectric sensing papers are insensitive to static force due to its physical limitation.[32]

Recently, a brand-new mechanism of pressure sensing, known as flexible iontronic sensing (FITS), has been introduced, which utilizes pressure-induced capacitive changes between electrodes and ionic surfaces.[27] Specifically, upon such an electronic-ionic contact, an interfacial electric double layer (EDL) is established immediately, possessing a particular supercapacitive property with an ultrahigh unit area capacitance (UAC) of up to several μF cm^{-2} in a sub-MHz spectrum.[33–35] As a comparison, the measured values of a typical parallel plate capacitive sensors are only within tens to hundreds of pF cm^{-2} in similar dimensions.[30] The measured EDL capacitance is proportional to the contact area between the electrodes and the ionic surfaces, which can be directly related to the external pressure load and induced mechanical deformation. In principle, both of the EDL capacitance and parallel-plate capacitance would contribute to the overall capacitive changes in the iontronic sensor.[33,39] However, the parallel-plate capacitance is on the order of several pF, while the interfacial EDL capacitance is on the order of tens to hundreds of nF. Therefore, the parallel-plate capacitance can be negligible in the measurement in a typical iontronic sensing device. Notably, unlike the conventional resistive and capacitive sensing modalities, the iontronic pressure sensor, based on the unique FITS mechanism, has shown extremely high sensitivity and resolution, while the parasitic noises can be largely negligible, given its ultrahigh signal-to-noise ratio (SNR).[33,35] As the key to generate the ionic-electric sensing interface, the liquid-phase ionic materials have been initially included, such as aqueous or organic electrolytes, and ionic liquids (ILs). They exhibit relatively high ion mobility and thus induce high EDL capacitance,[33] however, the evaporation of liquid, the poor structural stability and the complexity of the preparation process limit their applications. Recent advances in solid phase ionic materials, particularly found in energy and battery applications, such as ionic gels, hydrogels, polyelectrolytes, etc., offer higher structural stability, lower evaporation rate and lower leakage risk as compared to their liquid counterparts. Up-to-date, several types of iontronic sensing devices have been reported. For instance, iontronic droplet pressure sensors and iontronic film pressure sensors have been developed with optical transparency and high sensitivity to both normal and shear contact forces for emerging flexible sensing applications.[33,37,38] Moreover, the recently reported iontronic fabric sensors and iontronic-skin interface have both been utilized for long-term wearable health monitoring.[36,39,40] Notably, the iontronic pressure sensors address several major challenges of the conventional resistive, triboelectric and capacitive sensors, including low device sensitivity, vulnerability to environmental noises, no static response, optical opaqueness, etc.

In this paper, we have first introduced a single-sheet iontronic paper substrate with both ionic and conductive patterns as an all-in-one flexible sensing platform, which has extended the iontronic sensing principle to a more adaptive material system, with direct printability, custom cuttability, and 3D foldability at a low cost. Particularly, the iontronic sensing paper (ISP) devices can be structured into pressure/force sensing devices only by paper-specific manipulations, such as printing, cutting, folding, and gluing, in the forms of a simple 2D flexible device or a 3D tactile sensing-enabled origami. The pressure sensing mechanism of the ISP device is illustrated in **Figure 1**a, the applied pressure can cause an increment in the contact area among the conductive and ionic cellulose fibers, leading to a rise in the overall EDL capacitance of the device. As a result, the all-in-one ISP devices have shown a sensitivity greater than 10 nF kPa^{-1} cm^{-2} within a wide pressure range, a single-Pascal pressure resolution of 6.25 Pa, a millisecond mechanical response, and an adjustable measurement range up to 100 kPa. Importantly, the pressure-to-capacitance relationship in the sensitivity measurement shows a highly linear trend ($R^2 > 0.996$), which ensures a high sensitivity measurement to an extended pressure range of 25 kPa. To optimize such a desired device performance, a theoretical electromechanical model, based on the fibrous nonwoven nature of the paper and the unique iontronic interfacial capacitance, has been established to analyze the sensing responses of the ISP device. As demonstration of the high flexibility and broad adaptability of the all-in-one ISP concept, an array of ISP-enabled sensing applications has been implemented, including a weight-measuring iontronic origami box, an iontronic origami piano with a pressure-activated keyboard, an iontronic paper-formed wristband to capture human vital signals, as well as an iontronic paper matrix of 16×16 units to trace and map calligraphy.

2. Theoretic Model

To predict the theoretical capacitive changes under various pressure loads, an electromechanical model of the ISP device has been proposed. The contact area between ionic and conductive regions needs to be first assessed, to which the resulted EDL capacitance is directly proportional, given the UAC considered as a constant. The challenge is to calculate the contact area between the ionic and conductive regions with highly fibrous structures under different pressure loads (P). According to the classical compression theory of a fibrous assembly, the pressure-induced bending of the individual fibers causes the change in the volume fraction of the fibers (V_f) in the assembly, and successively affects the variation of the area fraction of the fibers at interfaces. As a result, it produces a corresponding capacitive change (C) of the ISP device.[39,41–43] An analytical equation between the capacitive change and the applied pressure can be derived accordingly

$$C = c_0 \cdot \frac{A}{6\pi V_{f0}^2} \cdot \frac{P}{KE} \tag{1}$$

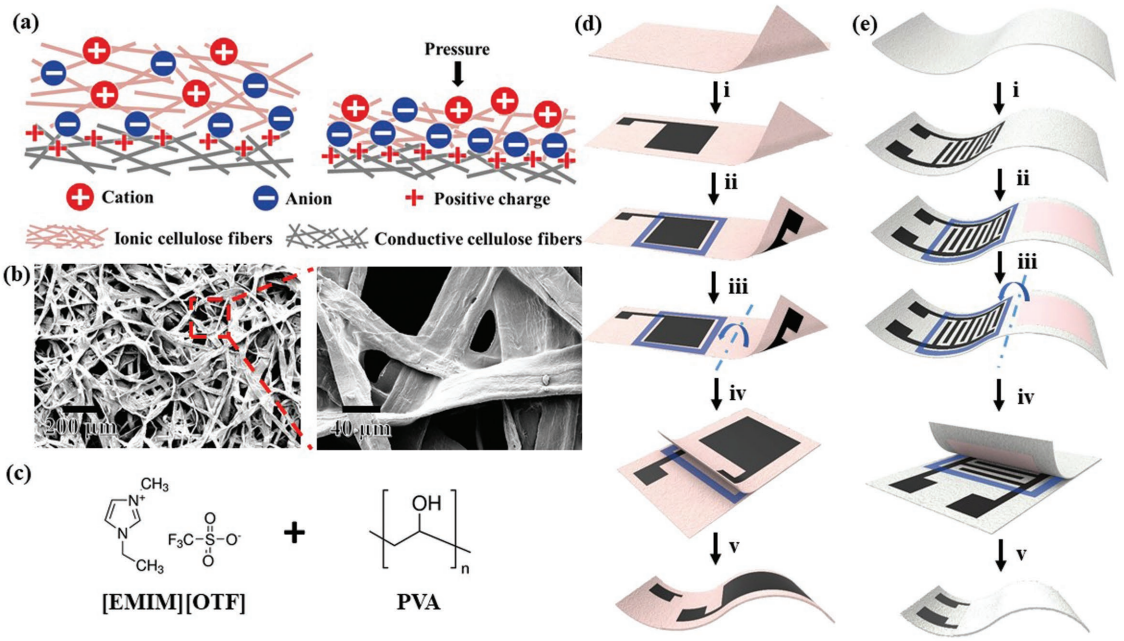

Figure 1. a) The pressure-response mechanism of the iontronic pressure sensing paper (ISP) device in which the fibrous ionic fibers is used as the ionic region and the conductive fibers is used as the conductive region; b) the SEM images of the ionic region of the ISP; c) illustration of the molecular structures of the ionic liquid and the polymer matrix: 1-ethyl-3-methylimidazoliumtrifluoromethanesulfonate and polyvinyl alcohol; d) the preparation of the ISP device with a sandwich structure: i) printing a top electrode onto the ionic paper, ii) printing a bottom electrode on the back side of the ionic paper, iii) printing adhesive patterns to integrate, iv) folding over to form the sandwich structure, v) final packaging and integration; e) the preparation of the ISP device with a bilayer structure: i) printing interdigital electrodes on a regular paper, ii) printing ionic ink onto the designed region, iii) printing adhesive patterns to integrate, iv) folding over to form the bilayer structure, v) final packaging and integration.

where c_0 stands for the UAC of the ISP, A denotes the sensing area, and V_{f0} means the initial volume fraction of the fibers assembly at zero pressure. Moreover, E represents the Young's modulus of the fiber material and K is a constant related to the force distribution on the fibers and can be derived from a classic bending formula of a simply supported beam from the literature.[46,47] Notably, this equation is only applicable when $P/KE \ll 1$ (the detailed derivation of this equation can be found in the Supporting Information). As can be seen, the capacitance of the ISP device has a linear relationship with the sensing area (A), the pressure applied (P), and the UAC of the ISP (c_0). Whereas, the elastic modulus of the fiber (E) and the initial fiber volume fraction (V_{f0}) show inverse influences on the sensitivity of the ISP device, that is, a softer fiber assembly or a fiber assembly with a lower initial volume fraction will lead to a higher device sensitivity with a greater change in area fraction under the same load.

3. Results and Discussions

3.1. The Microstructure, Preparation, and Materials of the Ionic Region of the ISP

Specifically, the ISP is comprised of both ionic and conductive patterns, leading to the formation of a free-standing functional composite substrate, from which the unique supercapacitive iontronic interfaces can be established only using the paper-specific manipulations. The ionic region of the ISP is a composite of cellulose fibers infused with an ionic content, of which the former supporting the porous structure of the ISP and the latter attaching onto the fibrous surface and providing the ionic property, as shown in the scanning electron microscopic (SEM) image in Figure 1b. Two methods have been presented here to prepare the ionic regions of the ISP: the first approach is to synthesize an ionic paper substrate from an ionic pulp solution and the second one utilizes an ionic ink to print onto a regular paper substrate. In particular, the preparation of the ISP by the ionic pulp starts from dispersing nature celluloses from wood, a classical fibrous material used in paper synthesis, into water to form a pulp solution. Polyvinyl alcohol (PVA), as a common biocompatible and biodegradable additive, is added to the pulp to improve the adhesion among the cellulose fibers. Afterward, a hydrophilic ionic liquid, 1-ethyl-3-methylimidazoliumtrifluoromethanesulfonate ([EMIM][OTF]), is introduced to the pulp as the ionic donor (Figure 1c). [EMIM][OTF] has been selected because it is a nontoxic water-soluble room temperature ionic liquid, whereas common ionic liquids using $[PF_6]^-$ or $[BF_4]^-$ as anions show extremely high toxicity for the generation of HF in water, and the ionic liquids using $[TFSI]^-$ as anions are not water soluble.[44] [EMIM][OTF] tends to disperse in PVA matrix to form an ionic gel for their similar solubility parameter (25.4 $MPa^{0.5}$ for [EMIM][OTF] and 25.8 $MPa^{0.5}$ for PVA) and polarity.[45,46] After the removal of the aqueous content by evaporation, the ionic liquid molecules are expected to be uniformly dispersed into the polymer matrix of PVA and form an ionic gel layer coated on the cellulose fibrous network, i.e., the ionic paper. The alternative method is to form a printable

ionic ink with a proper viscosity by dissolving PVA into an aqueous phase with the ionic liquid of [EMIM][OTF] at a predetermined ratio. Once, the ionic ink is dispensed onto a regular paper substrate through either inkjet printing or screen printing, the aqueous-dissolving ionic contents will penetrate the fibrous substrate and form an ionic shield on the cellulose fibers after a curing step, thus leading to the patterned ionic region of the ISP. The detailed illustration for the formations of the ionic regions can be found in Figure S1 (Supporting Information). The microfibrous structures of the ISP on one hand offer an extremely low contact area between ionic and conductive regions of the ISP at zero load, leading to an ultra-low initial value; on the other hand, it provides a large range of increase in the EDL capacitance as the external pressure rises at the ionic-electronic interfaces.

3.2. The Sensing Structures of the ISP Devices

As an all-in-one flexible sensing platform, ISP has also contained sensing electrodes made by conductive patterns, which, along with the ionic regions, and can be structured into several flexible pressure/force sensing architectures only using paper-specific manipulations, such as cutting, folding and gluing. As a result, it can lead to a formation of a sandwiched sensing structure with parallel electrodes, or a bilayer sensing structure with interdigitated electrodes. In particular, the sandwich-structured ISP device implements the electrode designs on both sides of the ionic paper. Following a specific folding operation, the printed electrodes can be folded over and overlapped with each other, and thereafter the sandwiched sensing paper can be structured into a single functional device, as shown in Figure 1d and the photo of the prepared device is shown in Figure S2a (Supporting Information). Whereas, the bilayer architecture of the ISP device can be directly achieved by using a regular paper substrate. Through consecutive printing processes, conductive and ionic inks along with adhesive can be dispensed into designated interdigitated electrodes, ionic and adhesive regions, respectively. Similarly, the multi-component containing ISP structure can be folded into a sensing device with a face-to-face contact between the interdigital electrodes and the ionic region, as exhibited in Figure 1e and the photo of the prepared ISP device is shown in Figure S2b (Supporting Information). It is worth noting that the two ISP architectures offers their own distinct advantages. Specifically, the sandwiched structure offers a higher device sensitivity with a higher units density, and can be shaped into any desired geometry by a simple cutting step, while the bilayer one can be applicable to different kinds of paper substrates, such as regular printing paper, heavy-duty cardboard paper, soft tissue paper, ultrafine filtering paper, and etc., as long as they are compatible with the inkjet and screen-printing processes of ionic and conductive inks, and can be designed into a more complicated ISP device by 3D origami process.

3.3. The Unit Area Capacitance of the Ionic Region of the ISP

As a key parameter in the iontronic sensing model, the UAC, which is directly proportional to the sensitivity of the ISP device,[39] has been defined as the measured capacitance of the ionic-electronic contact; in this case, that is the contact between unit area (cm^2) ionic and conductive regions of the ISP under an extremely high pressure (50 Mpa), that is, the nominal full contact. Figure 2a summarizes the UAC measurements at different frequencies using the ISPs prepared with different chemical formulas and preparation methods. All the ISP devices are prepared by ionic paper pulp except the printed ISP ones, which are prepared by printing ionic ink onto the paper prepared by the same paper pulp without ionic materials. As expected, the UAC decreases with the rise of the scanning frequency, similar to the capacitance-frequency dependence of supercapacitors, which is also established by ionic-electronic EDL.[34] Furthermore, the ISP exhibits a higher UAC when prepared with a higher ionic liquid concentration. For instance, the UACs of the ISPs increase from 0.066 to 6.47 and then to 25.7 μF cm^{-2} at 1000 Hz, when the weight ratio of cellulose fiber (CF) to IL changes from 1:0.25, 1:1, to 1:4. This can be explained by the classic Gouy–Chapman–Sterm model, in which the IL concentration is related to the Debye length of the electrolyte. A higher IL concentration leads to a reduced Debye length, and therefore, the ISP offers a higher UAC.[47,48] Moreover, the ionic patterns prepared by the two different methods, i.e., the pulp-made ISP and the ink printed-ISP, have only shown marginal differences in UAC values (6.47 μF cm^{-2} vs 5.93 μF cm^{-2}), indicating that the ionic property of the ISP mainly attribute to the composition of the ionic materials.[48]

3.4. The Capacitance-to-Pressure Properties of the ISP Devices

Several key device parameters can be extracted from the capacitance-to-pressure curves of the ISP devices, of which the slop rate leads to the device sensitivity . For a typical transducer, its device sensitivity has been conventionally defined as the output versus input signals. In the pressure sensor case, it is a ratio of the electric output to the pressure input.[49] For the iontronic sensing scheme, it offers remarkable improvements in the device sensitivity and base capacitance compared with parallel plate capacitive one, enabling direct capacitance measurement with a simplified circuit architecture, instead of assessing the normalized change of capacitance measured by a bridge circuitry. Therefore, in our ISP system, the unit of nF kPa^{-1} becomes suitable to evaluate the sensitivity performance of the iontronic devices recently.[30,50,51] In this study, by introducing a unit area confinement, we can compare different chemical formulations, different physical parameters of the ISP and two types of sensing architectures in a unified experimental platform, as the device sensitivity of ISP is directly proportional to the contact area, analogous to the physical definition of the UAC.[52] As a result, derived from Equation (1), the device sensitivity can be expressed as

$$\text{Sensitivity} = C/AP = \frac{c_0}{6K\pi V_{f0}^2 E} \tag{2}$$

3.4.1. The Influences of the Chemical Composition of the Ionic Region of the ISP

In order to validate the ISP sensing theory derived above, we conducted a series of characterization experiments using different ISPs with varying chemical and geometric parameters.

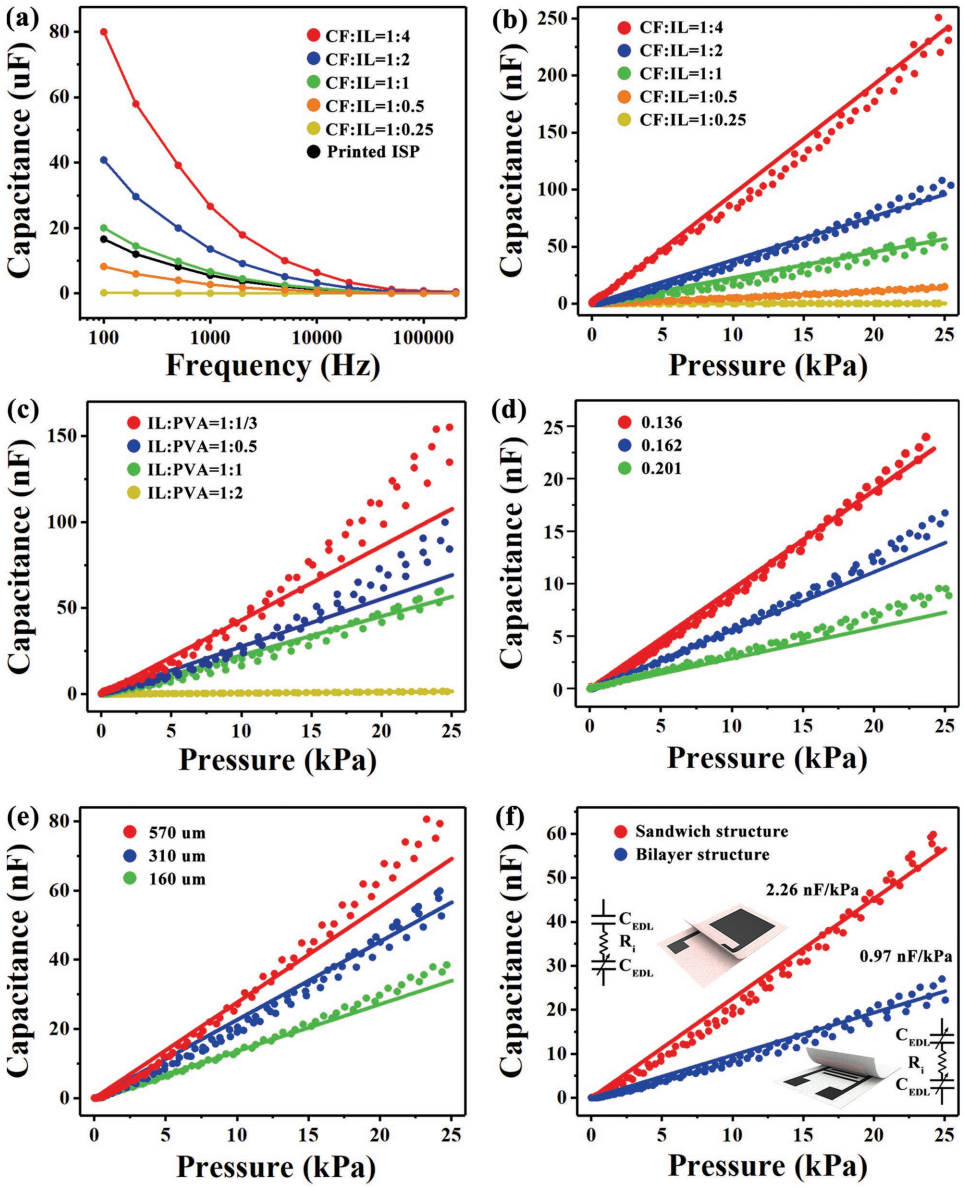

Figure 2. a) The measurement of the unit area capacitance (UAC) over interrogation frequencies of the ionic region of the ISP, the black curve/dots represent the UAC of the ISP prepared by printing ionic ink, while the other-colored curves/dots show the UAC of the ISPs prepared by paper pulp; b) experimental capacitance-pressure values (dots) and theoretic simulations (lines) of the ISP devices using the ISPs with different IL concentrations, ISPs are prepared by paper pulp; c) experimental capacitance–pressure data (dots) and theoretic curves (lines) of the ISP devices using the ISPs with different weight ratios between IL and PVA, ISPs are prepared by paper pulp; d) experimental capacitance–pressure values (dots) and theoretical simulations (lines) of the ISP devices using the ISPs with different initial volume fractions of the fibers, ISPs are prepared by paper pulp; e) experimental capacitance–pressure values (dots) and theoretic simulations (lines) of the ISP devices using the ISPs with different thicknesses, ISPs are prepared by paper pulp; f) experimental capacitance–pressure values (dots) and theoretic simulations (lines) of the ISP devices with different structures, the sandwich-structured device use the ISP prepared by paper pulp while the bilayer one use the ISP prepared by printing.

Figure 2b summarized the mechanical-to-capacitive characteristics of the sandwich-structured devices using the pulp-made ISPs with different IL concentrations, in which the measured capacitive values were plotted as dotted points, whereas the theoretical simulations were drawn as continuous lines. It was observed that the IL concentration in the ISPs had a significant influence on the sensitivity of the ISP device as it affected the UAC (c_0) of the ISP as well as the constant (K) in the equation. In particular, the ISP device with an optimal UAC value of 26.7 μF cm^{-2} had a device sensitivity of around 10 nF kPa^{-1} cm^{-2} within the detection range. And moreover, the ISP device with a higher ratio of the ionic content would result in a higher UAC, as well as a higher sensitivity. Figure 2c illustrated the capacitance-pressure curves of the sandwich-structured devices using the pulp-made ISPs with different ratios between IL and PVA, while the IL concentration in the ISP remains unchanged. The ISP with a higher weight ratio between IL and PVA has a higher UAC (3.34, 6.47, 51.9, and 104 μF cm^{-2} for the ISPs with weight

ratios between IL and PVA change from 1:2, 1:1, 1:0.5 to 1:1/3), but leads to an upward deviation with linear theoretical curve if the ratio is higher than 1:1. As pressure will cause the exudation of solvent in the gel, excess IL in PVA-IL gel will be released under pressure and increases the UAC as the pure IL exhibits a higher UAC (of 340 μF cm^{-2} at 1000 Hz) than the gel format.[53] To ensure the high linearity of the curve, the ratio between IL and PVA in ISP should be no higher than 1:1.

3.4.2. The Influences of the Initial Volume Fraction of the Fibers and the Thickness of the Ionic Region of the ISP

Figure 2d plotted the experimental investigations on the influence of the initial volume fraction (V_{f0}) of the fibers on the pulp-made ISP sensing performance. A mechanical fixture was used to apply pressure on the same ISP to achieve different V_{f0} while keeping other parameters, such as c_0 and K, unchanged. As expressed in Equation (1), a lower V_{f0} of the ISP led to a higher device sensitivity, as it is easier to compress a loose fiber assembly with a high ratio of voids. Well matched with the theoretical simulations, the ISP device with a V_{f0} of 0.201 showed a particular sensitivity of 0.36 nF kPa^{-1} cm^{-2}, which was 56% and 39% of that from the ones with V_{f0} of 0.162 and 0.136. Figure 2e showed the mechanical-to-capacitive responses of the devices using the pulp-made ISPs with different thicknesses, while their V_{f0} and K are thought to be the same. Thicker ISP leads to a higher sensitivity of the ISP device for the increase of the UAC of the ISP (The UAC of the ISP increases from 3.94 to 6.47 and then to 8.05 μF cm^{-2} at 1000 Hz, when the thickness of the ISP rises from 160um, 310um to 570um), as thicker ISP contains more mobile ion, therefore the UAC of the ISP is higher for more ion existed at electrode/ionic paper interfaces.

As illustrated in Equation (2), the initial volume fractions (V_{f0}) play a dominant role in determining the device sensitivity, as it follows a quadratic relationship with the resulted capacitive values. However, along with K and E, it is an intrinsic property of the paper substrate, and may not be tunable easily.[42,43] Alternatively, the UAC (c_0) is the interfacial property determined by the ionic compositions of the ISP, which can be used to adjust the device sensitivity in practice, as shown in Figure 2b,c.

3.4.3. The Influences of the Structures of the ISP Devices

To explore the structural influence on the ISP devices, the two types of the ISP devices with the sandwich structure and bilayer structure have been compared side-by-side in Figure 2f. Provided with the identical chemical compositions and geometric parameters, the sandwich-structured ISP device using the ISP prepared by ionic pulp offers a sensitivity of 2.26 nF kPa^{-1} cm^{-2}, which is more than twice of that of the bilayer-structured counterpart (of 0.98 nF kPa^{-1}) using the ISP prepared by printing, even though the ionic regions prepared by the two methods present a marginal difference in UAC values (<10%) as shown in Figure 2a. This doubling value in the sensitivity measurement attributes to the structure-induced measurement differences. As illustrated, the ISP devices consist of two EDL capacitors connected in series. In the sandwich structure, one of the EDL capacitors has a greater value than that of the other as the electrode has been directly printed onto the ionic region. And therefore, the smaller pressure-sensing capacitor dominates in the capacitive measurement due to this type of the configuration. On the other hand, the bilayer-structured ISP has two equivalent variable capacitors connected in series, so the overall capacitance is reduced to half of the value of the interfacial capacitance. Therefore, it is expected that the device sensitivity is doubled in the sandwich-structured ISP devices

3.4.4. The Linearity of the Pressure-to-Capacitance Response and the Measurement Range of the ISP Devices

Another highly desirable feature of the ISP devices is the high linearity in its pressure-to-capacitance measurement, which can simplify the design of the measurement circuitry and produce consistent high-sensitivity readings. The linear correlation coefficients have been calculated to be 0.993 and 0.996 for the sandwich-structured and bilayer-structured ISP devices, respectively. Such a high linearity of the ISP device benefits from the iontronic sensing nature in which the capacitive measurement is proportional to the contact area change induced by external loads. Moreover, the high elastic modulus of the cellulose fiber (8–10 GPa)[31,54] satisfies the pressure-to-capacitance relation of the ISP within its linear limit ($P/KE \ll 1$), which can be extended to a greater pressure range up to 100 kPa (as shown in Figure S3, Supporting Information).

3.4.5. Bending Stability and Temperature Stability of the ISP Device

Moreover, we have characterized the bending dependence and temperature dependence of the ISP devices. The characterization of the capacitance changes of the sandwiched ISP devices prepared by the ionic pulp-made paper has been conducted by bending over the surfaces with varying radius of curvature, as shown in **Figure 3**a, given a fixed sensing area of 1 × 1 cm^2. Compared with the sensitivity of the ISP devices tested on a plate, only marginal drifts can be observed on the sensitivity curves of the same ISP device tested over a cylindrical objects with 100 mm radius of curvature, and about 10% and 25% increases in sensitivities of the device tested over the cylinders with 50 and 25 mm radii of curvature, suggesting a reliable performance of the ISP devices over various surface topologies. The temperature dependence of the ISP device has been summarized in Figure 3b, in which the measured capacitive values of the sandwiched ISP devices, under a constant pressure load of 50 kPa and the fixed sensing area of 1 × 1 cm^2, keep increasing at a nearly linear rate of 0.054 $°C^{-1}$, as the mobility of ions in ionic liquid or ionic gel rises with the temperature, which can be described by Vogel–Tamman–Fulcher (VTF) equation.[53,55]

3.5. The Response Time, Repeatability, and Minimal Pressure Resolution of the ISP Devices

Additional characterization tests were conducted to evaluate the mechanical response time, repeatability, reliability and

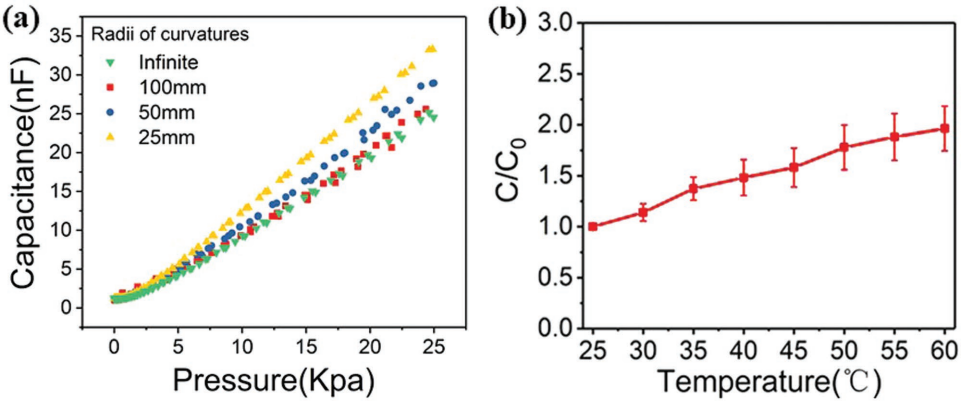

Figure 3. a) The pressure-to-capacitance responses of the sandwiched ISP devices prepared by the ionic pulp-made paper over various surface topologies of which the radius of curvature ranging from 25 mm to infinite; b) the measured capacitance versus temperature of the sandwiched ISP devices under a constant pressure load of 50 kPa (given a fixed sensing area of 1 × 1 cm^2).

minimal pressure resolution. The tests for the mechanical response were first carried out using a piezoelectric actuator to apply a periodical load (of approximately 80 Pa) onto the ISP devices,[39] the measurement results were summarized in **Figure 4**a. By evaluating the loading and unloading phases during each duty cycle, the response and reset times of the device were obtained as 5 and 4 ms, respectively, ensuring rapid responses to mechanical stimuli. This can be explained as the cellulose fibers possess relatively high Young's modulus (of 8–10 GPa), even though the ISP exhibited high flexibility. Moreover, the repeatability and reliability of the ISP device were characterized under repetitive pressure loads of 1, 5, and 10 kPa at 1 Hz, and the measurement results, summarized in Figure 4b, indicate that less than 5% variations in the magnitude have been observed after 1000 duty cycles, proving the long-time stability of the device under different loads. Given the high elastic modulus and strength of the cellulose fiber, the plastic deformation of the fibers could be insignificant under these loading conditions, resulting in a high stability and repeatability of the device, in addition to its rapid mechanical responses. At last, taking an advantage of the high noise immunity of the iontronic sensing mechanism, the ISP devices demonstrated high definition of the pressure resolution and a low detection limit, as shown in Figure 4c. A single Pascal level detection of an ultralight object (e.g., a cotton ball of 0.0625 g placed on an ISP device with 1*1 cm^2 sensing area) had been illustrated successfully, which was around 6.25 Pa.

3.6. Folded Pressure-Sensing Bracelet Origami for Pulse Wave Monitor

Foldability serves as one of the unique properties of the ISP devices. Using the well-established origami/paper-folding techniques, the ISP devices can be transformed from a 2D planar substrate into a 3D functional platform, combined with other paper-specific operations such as printing and gluing. As demonstrated in **Figure 5**a,b, a pressure-sensing bracelet origami can be shaped by alternating printing interdigital electrodes and ionic patterns on the designated areas of a regular paper substrate. Followed by the folding technique, it forms a bilayer-sensing device embedded into the bracelet origami. The pulse-waveform measurement is achieved by a gentle pressure applied onto the sensing area and the radial artery through a finger. The resulted origami ISP exhibits high sensitivity and high flexibility, and can be used as a simple wearable device for continuous pulse wave monitoring of blood pressure, enabling measurements of body vital signals, such as heart rates, respiratory rates, emotional stress and blood pressure variations, shown in Figure 5c.

3.7. Folded Piano Origami with Pressure-Sensing Keyboard

Furthermore, more sophisticated origami structures with multiplexed sensing devices can be designed and processed

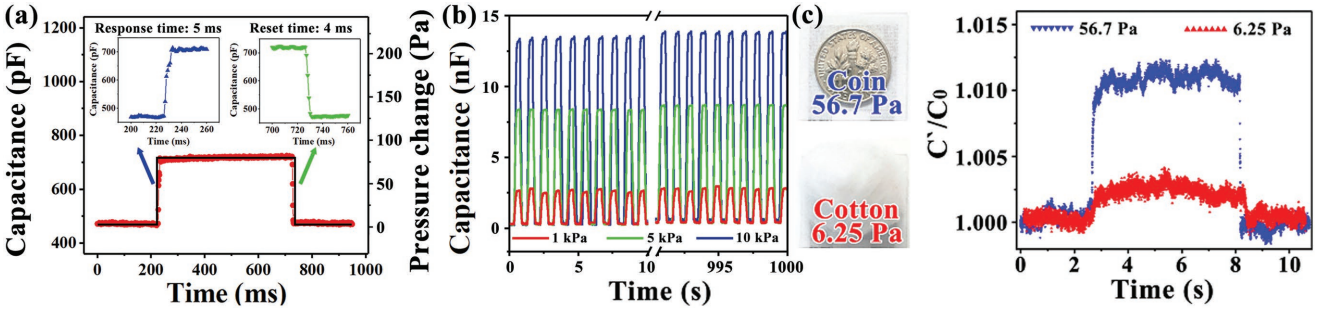

Figure 4. a) Response time and reset time of the ISP device; b) measurement stability of the ISP device under cyclic mechanical loads of 1 Hz; c) measured capacitance curve of the ISP device under ultralow pressure applied by a coin or a cotton ball.

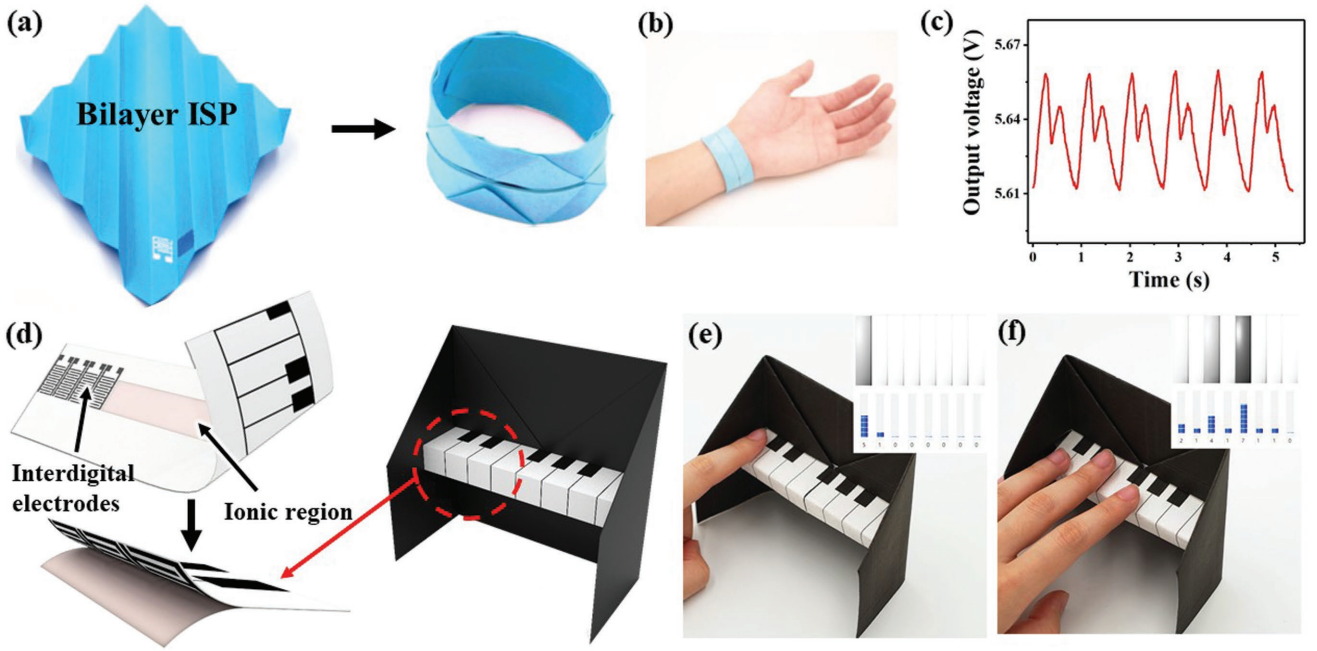

Figure 5. a) The preparation of the ISP origami bracelet using printing and folding; b) the ISP origami bracelet is wearable for pulse monitoring, c) the pulse wave signal collected by the ISP origami bracelet; d) the preparation of the ISP origami piano with pressure-sensitive keyboard; e,f) the ISP origami piano with force-sensing function can detect the pressure and control the volume.

with more refined conductive and ionic patterns along with additional folding steps. For instance, an electronic piano with pressure-sensitive eight keys has been achieved by the bilayer ISP origami architecture. Its preparation steps have been presented in Figure 5d, in which it likewise starts with ionic patterning and electrodes printing, respectively, followed by the color printing for the piano keys and constructs, the detailed steps are shown in Figure S4 (Supporting Information). Subsequent to the pre-designed folding steps, an electronic piano with 8-keys is ready to perform with driving electronics. Notably, it can differentiate more than 16 000 levels of pressure, in another word, the pressure resolution of the ISP device is up to 6.25 Pa, leading to a high-performance electronic keypad, shown in Figure 5e,f (along with the demo video in the Supporting Information). By introducing the printable and foldable ISP concept, one can enable multiplexed electronic feedbacks to the millennium-long origami conventions with new functionalities and technical features.

3.8. Pressure-Sensing Smart Pillbox for Weight Measurement

Cuttability is another distinct feature of the paper-based sensing platform, permitting diverse shapes to fit with various surfaces with different geometries. As Illustrated in **Figure 6**a,b, an ISP device has been prepared accordingly, using the sandwiched-sensing architecture, with its shape trimmed and folded into a circular container, for smart pillbox applications. In particular, the ISP includes a scissor-cut body structure to form a 3D pillbox, while on the other end, a circular-trimmed electrode along with an ionic-inked electrode are stacked over, forming the pressure-sensing structure of the smart ISP pillbox. The 3D ISP pillbox can distinguish the weight changes of the contained pills with subgram resolutions. For instance, when loaded with two different-weighted pills, the green pills of 0.62 g (corresponding distribution pressure is 15 Pa) and the white ones of 0.32 g (corresponding pressure is 8 Pa), the ISP pillbox can first estimate the number of pills of different species, and second, it can distinguish the pills with different weights, as shown in Figure 6c. Such an ISP-cutting means would enable inexpensive yet high-resolution detection of subtle pressure and weight changes on various shapes of objects or their packaging.

3.9. ISP Matrix for Pressure Mapping

Moreover, the sandwiched ISP architecture can be utilized to construct high-density pressure sensing matrix, as the top and bottom electrodes can be printed orthogonally on both sides of the paper substrate with patterned ionic region sandwiched in the middle layer and form a scanning electronic array. Specifically, a 16×16 sensing matrix using the sandwiched ISP architecture has been implemented with an additional adhesive layer to secure the top and bottom electrodes along with the ionic region, as shown in Figure 6d,e. The high-resolution pressure-sensing paper is particularly useful as a tracking and mapping tool during the brush-writing process of Chinese calligraphy. As shown in Figure 6f (along with the demo video in the Supporting Information), the ISP matrix paper not only continuously traces the handwriting, but also records the pressure magnitudes and patterns of the brush tips in a high-definition fashion, which are considered critically important for Chinese calligraphy.[56] Furthermore, the ISP matrix paper can also record the real-time pressure of any individual sensing unit

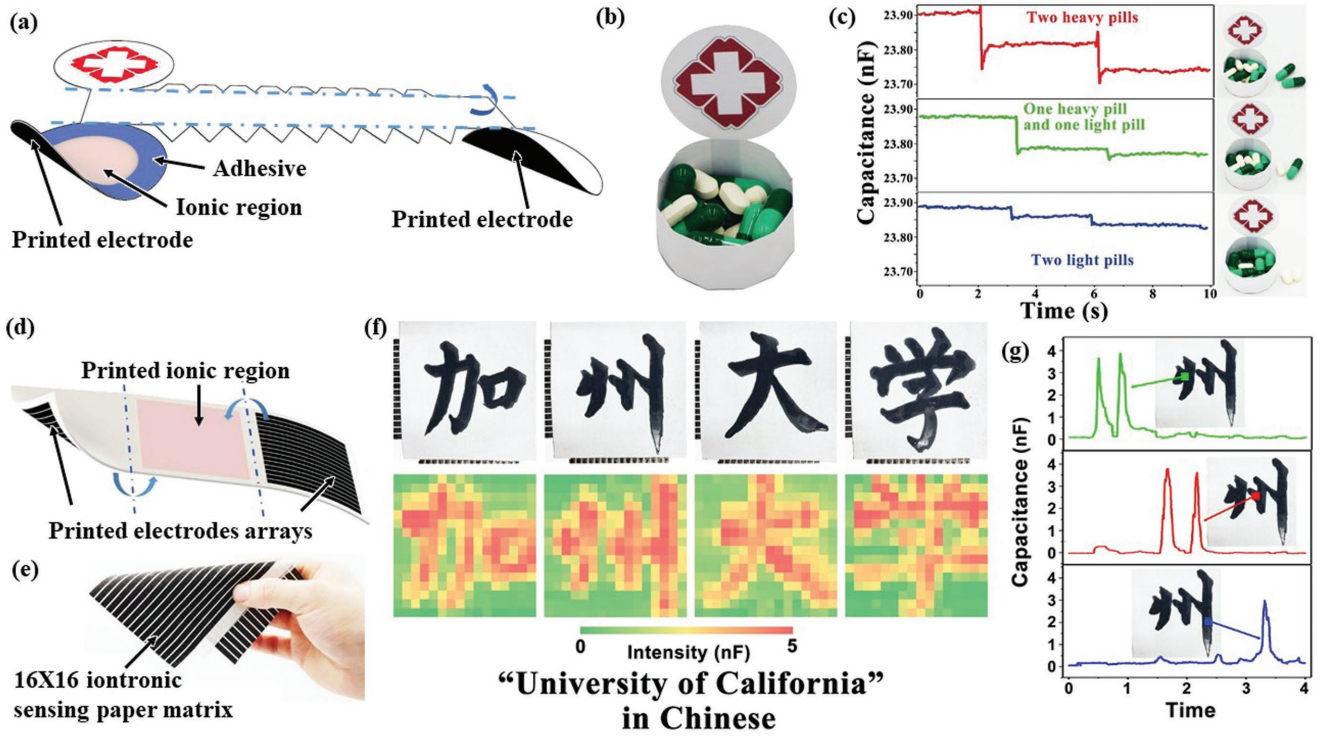

Figure 6. a,b) The preparation of the 3D pill box origami with weight-sensing ability; c) the ISP pill box can distinguish the number and weight of the pills taking out from it; d) the preparation of the 16*16 ISP matrix by printing electrodes array and ionic ink on designed regions of a common paper, followed by folding to achieve the e) 16*16 ISP matrix for pressure mapping, f) the tracking and mapping of the pressure during the brush-writing process of Chinese calligraphy; g) the real-time capacitance-time curves at different sensing units when writing one word.

during writing, which is important to identify the writing habits of different people. Moreover, it can turn the conventional one time-use special calligraphy paper into a reusable electronic ISP substrate with the detailed of the hand-writing arts recorded digitally. On the other hand, such a novel low-cost input device can be employed to recognize different writing patterns or habits as a biometric identification device for growing demands in encryption and decryption applications.[57]

4. Conclusion

In summary, the iontronic pressure-sensing paper prepared by ionic-containing materials and paper-specific operations, such as printing, cutting, folding, and gluing, has been established in an all-in-one fashion and demonstrated for various applications. Its paper matrix-nature derived from the history-long evolution allows it to be naturally flexible, structurable, disposable, and low cost. By simple paper-specific manipulations, one paper can be structured into a sandwich-structured ISP device with a higher sensitivity and shape-diversity, while a bilayer-structured ISP device has a thinner implementation and origami-accessibility. On the other hand, the iontronic sensing capacity of the ISP devices provides a high device sensitivity of 10 nF kPa^{-1}, a single Pascale resolution of 6.25 Pa, a rapid mechanical response of 4–5 ms, as well as a high linearity with $R^2 > 0.996$, in addition to its high repeatability. Notably, an electromechanical model has been built and a theoretical derivation has been validated to explain the capacitance-pressure behavior of the ISP device. Taking advantages of the cuttability, printability and foldability of the paper, the device can be cut into any shape and seamlessly integrated with objects or their packaging to detect the weight variations; the device can also be folded to structure a smart 3D origami with electronic interfaces, such as high-definition paper piano with high-level volume control and wearable origami bracelet for continuous monitoring of blood pulse waveforms. In addition, using the sandwiched ISP architecture, a 16×16 pressure sensing matrix can be prepared to trace and record the handwriting process and pressure distributions for Chinese calligraphy. Therefore, the proposed ISP devices represent an original smart paper concept enabled by the iontronic sensing principle with remarkable sensing advantages. It has shown an array of potential promising applications in the emerging fields, such as smart packaging, personal wearables, flexible human–machine interfaces, etc., where the device sensitivity, low cost, 3D structurability, and surface adaptability are all required.

5. Experimental Section

Preparation of the Ionic Region of the Iontronic Sensing Paper: 1) *Prepared by Paper Pulp*: Commercial paper fiber (nature microfiber cellulose (MFC) pulp, Qinghong Materials Inc.) was dispersed in water and stirred for 1 h to form a 1% wt paper pulp. According to the ionic materials concentration, different amounts of PVA (98–99% alcoholysis degree, Aladdin Reagent Company) and [EMIM][OTF] (98%,

Sigma-Aldrich) were added into the paper pulp with stirring. PVA was predissolved into water to form a 10% solution. Prepared paper pulp with ionic materials was poured into a 100 mm diameter glass petridish. Afterward, the paper pulp was dried at atmosphere at 100 °C to totally evaporate water. The ionic paper was thus prepared after peeling it off from the petridish.

2) *Prepared by Printing*: PVA was dissolved in water to form a 15% wt solution, then [EMIM][OTF] was added with a weight ratio of 1:1 with PVA, followed by stirring the solution for 30 min to form a uniform ink with relatively high viscosity. Screen printer was used to print the ionic ink on common paper. Here Chinese rice paper with thin thickness and good printability was chosen. After printing, the paper was dried at atmosphere at 100 °C for 30 min to evaporate water, therefore an ionic coating was formed on the designed area on the paper. The two methods to prepare the ionic region of the ISP are illustrated in Figure S1 (Supporting Information).

Device Fabrication: For single unit ISP device based on sandwich structure, carbon or silver paste was screen printed on the ISP to form a 1*1 cm^2 electrode, followed by printing another 1*1 cm^2 electrode on the back of the paper. Afterward, 15% wt PVA solution, as adhesive, was printed along the edge. Finally, the ISP was folded along the middle line between two electrodes to overlap the electrodes with each other. The device was connected with an flexible printed circuit (FPC) using anisotropic conductive tape. For the ISP device based on bilayer structure, carbon or silver paste was screen printed on the designed location of a Chinese rice paper to form the interdigital electrodes, then ionic ink was screen printed on the paper to form an ionic pattern. Folding the paper along the designed folding lines to ensure the face-to-face contact between the interdigital electrodes with the ionic region, the bilayer-structured ISP device was thus prepared.

Measurement Setup: The capacitance–pressure behaviors of the ISP devices were characterized by measuring the capacitance of the device under external pressure applied. The device with a 1*1 cm^2 sensing area was adhered on a moving stage (KMTS50E/M, Thorlabs), and pushed toward a dynamometer (M5-2, Mark-10) to get the pressure value. A 2*2 cm^2 soft silicone rubber (Ecoflex 00–10) was put between the ISP device and the measuring head of the dynamometer to distribute stress uniformly. The capacitance of the device was obtained by an inductance, capacitance, resistance (LCR) meter (Tonghui 2829C) at 1000 Hz and a sine input with a peak voltage of 500 mV, thus obtaining the capacitance–pressure curves of the devices. Mechanical response characterization of the sensor was conducted by driving a piezoelectric bender with a ±20 V peak-to-peak square wave to apply a periodic contact pressure to the device, and the real-time capacitance curve of the device was recorded by a data acquisition card (DAQ, NI USB-6361, NI Instruments Corporation). The stability test was conducted by the moving stage to periodically push toward and backward the device to a dynamometer, the capacitance curve was also recorded by the DAQ card. The readout circuitries for single unit sensing and matrix sensing is shown in Figure S5 (Supporting Information) and the test system for the 16*16 ISP matrix is shown in Figure S6 (Supporting Information).

Supporting Information

Supporting Information is available from the Wiley Online Library or from the author.

Acknowledgements

This research was supported by the Joint Research Fund for Overseas Chinese Scholars and Scholars in Hong Kong and Macao (51628502), the Shenzhen Fundamental Research Program (JCYJ20170413164102261), the Program for Guangdong Introducing Innovative and Entrepreneurial Teams (2016ZT06D631), and the National Key R&D Program of China (2017YFA0701303).

Conflict of Interest

Z. Zhu, R. Li, Y. Chang, and T. Pan are involved in startup companies that are developing wearable sensing technologies.

Keywords

iontronic, origami, paper electronics, pressure sensing, wearable electronics

Received: October 17, 2018
Revised: December 10, 2018
Published online:

[1] S. M. Z. Hossain, R. E. Luckham, A. M. Smith, J. M. Lebert, L. M. Davies, R. H. Pelton, C. D. M. Filipe, J. D. Brenan, *Anal. Chem.* **2009**, *81*, 5474.
[2] P. Das, A. Ghosh, H. Bhatt, A. Das, *RSC Adv.* **2012**, *2*, 3714.
[3] D. Nilsson, T. Kugler, P. Svensson, M. Berggren, *Sens. Actuators, B* **2002**, *86*, 193.
[4] N. Dossi, R. Toniolo, A. Pizzariello, E. Carrilho, E. Piccin, S. Battiston, G. Bontempelli, *Lab Chip* **2012**, *12*, 153.
[5] H. Andersson, A. Manuilskiy, T. Unander, C. Lidenmark, S. Forsberg, H. Nilsson, *IEEE Sens. J.* **2012**, *12*, 1901.
[6] J. W. Han, B. Kim, J. Li, M. Meyyappan, *J. Phys. Chem. C* **2012**, *116*, 22094.
[7] L. Wang, W. Chen, D. Xu, B. S. Shim, Y. Zhu, F. Sun, L. Liu, C. Peng, Z. Jin, C. Xu, N. A. Kotov, *Nano Lett.* **2009**, *9*, 4147.
[8] W. He, Y. Sun, J. Xi, A. A. M. Abdurhman, J. Ren, H. Duan, *Anal. Chim. Acta* **2016**, *903*, 61.
[9] D. Kong, L. Liu, S. Song, S. Suryoprabowo, A. Li, H. Kuang, L. Wang, C. Xu, *Nanoscale* **2016**, *8*, 5245.
[10] Y. Ma, H. Li, S. Peng, L. Wang, *Anal. Chem.* **2012**, *84*, 8415.
[11] S. Yun, J. Kim, *Sens. Actuators, B* **2010**, *150*, 308.
[12] S. M. Z. Hossain, J. D. Brenan, *Anal. Chem.* **2011**, *83*, 8772.
[13] J. Lu, S. Ge, L. Ge, M. Yan, J. Yu, *Electrochim. Acta* **2012**, *80*, 334.
[14] S. Ge, L. Ge, M. Yan, X. Song, J. Yu, J. Huang, *Chem. Commun.* **2012**, *48*, 9397.
[15] A. J. Gimenez, J. M. Y. Limon, J. M. Seminario, *J. Phys. Chem. C* **2011**, *115*, 282.
[16] M. Nogi, M. Karakawa, N. Komoda, H. Yagyu, T. T. Nge, *Sci. Rep.* **2015**, *5*, 17254.
[17] L. Yuan, B. Yao, B. Hu, K. Huo, W. Chem, J. Zhou, *Energy Environ. Sci.* **2013**, *6*, 470.
[18] G. Zheng, L. Hu, H. Wu, X. Xie, Y. Cui, *Energy Environ. Sci.* **2011**, *4*, 3368.
[19] L. Hu, J. W. Choi, Y. Yang, S. Jeong, F. L. Mantia, L. F. Cui, Y. Cui, *Proc. Natl. Acad. Sci. USA* **2009**, *106*, 21490.
[20] L. Hu, Y. Cui, *Energy Environ. Sci.* **2012**, *5*, 6423.
[21] M. Agarwal, Q. Xing, B. S. Shim, N. Kotov, K. Varahramyan, Y. Lvov, *Nanotechnology* **2009**, *20*, 215602.
[22] L. Tao, K. N. Zhang, H. Tian, Y. Liu, D. Y. Wang, Y. Q. Chen, Y. Yang, T. L. Ren, *ACS Nano* **2017**, *11*, 8790.
[23] M. A. Kafi, A. Paul, R. Dahiya, presented at *IEEE Sensors 2017*, Glasgow, UK **2017**, https://doi.org/10.1109/ICSENS.2017.8234441.
[24] Q. Zhong, J. Zhong, B. Hu, Q. Hu, J. Zhou, Z. L. Wang, *Energy Environ. Sci.* **2013**, *6*, 1779.
[25] S. Gong, W. Schwalb, Y. Wang, Y. Chen, Y. Tang, J. Si, B. Shirinzadeh, W. Cheng, *Nat. Commun.* **2014**, *5*, 3132.
[26] A. Chortos, J. Liu, Z. N. Bao, *Nat. Mater.* **2016**, *15*, 937.
[27] J. Herkenfeld, A. Jajack, J. Rogers, P. Gutruf, L. Tian, T. Pan, R. Li, M. Khine, J. Kim, J. Wang, J. Kim, *Lab Chip* **2018**, *18*, 217.

[28] O. Atalay, A. Atalay, J. Gafford, C. Walsh, *Adv. Mater. Technol.* **2018**, *3*, 1700237.
[29] S. Takamatsu, T. Kobayashi, N. Shibayama, K. Miyake, T. Itoh, *Sens. Actuators, A* **2012**, *184*, 57.
[30] D. J. Lipomi, M. Vosgueritchian, B. C. K. Tee, S. L. Hellstrom, J. A. Lee, C. H. Fox, Z. N. Bao, *Nat. Nanotechnol.* **2011**, *6*, 788.
[31] N. Jonassen, presented at *Electrical Overstress/Electrostatic Discharge Symp. Proc.*, Reno, Nevada, USA, October **1998**.
[32] F. R. Fan, L. Lin, G. Zhu, W. Wu, R. Zhang, Z. L. Wang, *Nano Lett.* **2012**, *12*, 3109.
[33] B. Nie, R. Li, J. Cao, J. D. Brandit, T. Pan, *Adv. Mater.* **2015**, *27*, 6055.
[34] K. H. Lee, M. S. Kang, S. Zhang, Y. Gu, T. P. Lodge, C. D. Frisbie, *Adv. Mater.* **2012**, *24*, 4457.
[35] B. Nie, R. Li, J. D. Brandit, T. Pan, *Lab Chip* **2014**, *14*, 1107.
[36] M. L. Jin, S. Park, Y. Lee, J. H. Lee, J. Chung, J. S. Kim, J. S. Kim, S. Y. Kim, E. Jee, D. W. Kim, J. W. Chung, S. G. Lee, D. Choi, H. T. Jung, D. H. Kim, *Adv. Mater.* **2017**, *29*, 1605973.
[37] B. Nie, S. Xing, J. D. Brandt, T. Pan, *Lab Chip* **2012**, *12*, 1110.
[38] B. Nie, R. Li, J. D. Brandt, T. Pan, *Lab Chip* **2014**, *14*, 4344.
[39] R. Li, Y. Si, Z. Zhu, Y. Guo, Y. Zhang, N. Pan, G. Sun, T. Pan, *Adv. Mater.* **2017**, *29*, 1700253.
[40] Z. Zhu, R. Li, T. Pan, *Adv. Mater.* **2018**, *30*, 1705122.
[41] J. Hu, *Structure and Mechanics of Woven Fabrics*, CRC Press LLC, USA **2004**.
[42] C. M. V. Wyk, *J. Text. Inst.* **1946**, *37*, T285.
[43] N. Pan, *J. Compos. Mater.* **1994**, *28*, 1500.
[44] P. Scovazzo, J. Kieft, D. A. Finan, C. Koval, D. Dubois, R. Noble, *J. Membr. Sci.* **2004**, *238*, 57.
[45] K. Swiderski, A. Mclean, C. M. Gordon, D. H. Vaughan, *Chem. Commun.* **2004**, *19*, 2178.
[46] H. Du, J. Zhang, *Soft Matter* **2010**, *6*, 3370.
[47] O. Stern, *Z. Elektrochem.* **1924**, *30*, 1014.
[48] M. Kappl, *Surface and Interfacial Forces*, Wiley-VCH, Weinheim, Germany **2009**.
[49] Q. Cheng, S. Wang, *Composites, Part A* **2008**, *39*, 1838.
[50] S. H. Lee, S. Wang, G. M. Pharr, M. Kant, D. Penumadu, *Holzforschung* **2007**, *61*, 254.
[51] R. W. Koppelaar, *Bachelor Dissertation*, Eindhoven University of Technology, Mechanical Engineering, **2009**.
[52] J. J. Carr, J. M. Brown, *Introduction to Biomedical Equipment Technology*, 3rd ed., Prentice Hall, New Jersey **2001**.
[53] M. A. B. Susan, T. Kaneko, A. Noda, M. Watanabe, *J. Am. Chem. Soc.* **2005**, *127*, 4976.
[54] G. Schwartz, B. C. K. Tee, J. Mei, A. L. Appleton, D. H. Kim, H. Wang, Z. Bao, *Nat. Commun.* **2013**, *4*, 1859.
[55] J. Vila, P. Gines, J. M. Pico, C. Franjo, E. Jimernez, L. M. Varela, O. Cabeza, *Fluid Phase Equilib.* **2006**, *242*, 141.
[56] Y. Chiang, *Chinese Calligraphy: An Introduction to Its Aesthetic and Technique*, 3rd ed., Harvard University Press, Cambridge, MA **1972**.
[57] S. Hoque, M. Fairhurst, G. Howells, presented at *ECSIS Symposium on IEEE*, IEEE, Edinburgh, UK, August **2008**, pp. 17–22, https://doi.org/10.1109/BLISS.2008.8.